

# Study on seismic retrofit of structures using SPSW systems and LYP steel material

Tadeh Zirakian<sup>\*1</sup> and Jian Zhang<sup>2</sup>

<sup>1</sup>*Department of Civil Engineering and Construction Management,  
California State University, Northridge, CA, USA*

<sup>2</sup>*Department of Civil and Environmental Engineering, University of California, Los Angeles, CA, USA*

*(Received January 7, 2015, Revised August 5, 2015, Accepted November 27, 2015)*

**Abstract.** Steel plate shear walls (SPSWs) have been shown to be efficient lateral force-resisting systems, which are increasingly used in new and retrofit construction. These structural systems are designed with either stiffened and stocky or unstiffened and slender web plates based on disparate structural and economical considerations. Based on some limited reported studies, on the other hand, employment of low yield point (LYP) steel infill plates with extremely low yield strength, and high ductility as well as elongation properties is found to facilitate the design and improve the structural behavior and seismic performance of the SPSW systems. On this basis, this paper reports system-level investigations on the seismic response assessment of multi-story SPSW frames under the action of earthquake ground motions. The effectiveness of the strip model in representing the behaviors of SPSWs with different buckling and yielding properties is primarily verified. Subsequently, the structural and seismic performances of several code-designed and retrofitted SPSW frames with conventional and LYP steel infill plates are investigated through detailed modal and nonlinear time-history analyses. Evaluation of various seismic response parameters including drift, acceleration, base shear and moment, column axial load, and web-plate ductility demands, demonstrates the capabilities of SPSW systems in improving the seismic performance of structures and reveals various advantages of use of LYP steel material in seismic design and retrofit of SPSW systems, in particular, application of LYP steel infill plates of double thickness in seismic retrofit of conventional steel and code-designed SPSW frames.

**Keywords:** steel plate shear walls; low yield point steel; seismic retrofit; nonlinear time-history analysis; seismic demand

## 1. Introduction

There are many seismically vulnerable existing buildings which are not designed in accordance with the modern seismic codes, and hence are susceptible to exhibit weak performance and undergo failure when subjected to earthquake excitations. The lateral force-resisting systems of such buildings are typically retrofitted using steel braces, steel plates, and reinforced concrete shear walls for improved structural and seismic performance.

---

<sup>\*</sup>Corresponding author, Ph.D., E-mail: [tadeh.zirakian@csun.edu](mailto:tadeh.zirakian@csun.edu)

Some retrofitting systems are becoming more favorable based on their performance, construction and implementation costs, ease of implementation, availability of material, and minimum disruption to the function as well as occupants of the building. On this basis, the use of bulky retrofitting systems, e.g., reinforced concrete shear walls, becomes more limited due to the complications in erection and high costs for foundation, while the application of lighter retrofitting systems such as steel braces and shear walls has become relatively more favorable (Dung 2011).

In addition to new construction, steel plate shear wall (SPSW) systems have been increasingly used in the seismic retrofit of existing building structures due to the various advantages they offer compared to other lateral force-resisting systems. Mahtab and Zahedi (2008) have demonstrated the relative superiority of steel shear walls to steel cross braces in retrofitting of a 10-story structure. Moreover, Park *et al.*'s (2007) test results have shown that unlike conventional reinforced concrete walls and braced frames, well-designed steel plate walls exhibit high strength and large ductility as well as energy dissipation capacity. In addition, due to the exceptional hysteretic behavior and the capability to early undergo plastic deformations, low yield metal shear panels have also been conceived as hysteretic dampers which could be profitably used as new methodology for the seismic retrofitting of existing steel and concrete structures (Mistakidis *et al.* 2007).

In addition to the reported studies on the structural behavior and seismic performance of SPSW systems especially with low yield point (LYP) steel infill plates, nonlinear and inelastic dynamic response of SPSW systems has also been investigated by some researchers. For instance, Rezai (1999) reported experimental and analytical studies on the behavior of SPSWs under cyclic and dynamic loadings. In addition, Bhowmick (2009), Bhowmick *et al.* (2009), Kurban (2009), Kurban and Topkaya (2009), Berman (2011) studied the dynamic response and characteristics of SPSW systems through nonlinear time-history analyses and provided interesting and effective results. However, a search of the literature reveals that apart from the aforementioned studies and also some additional scattered investigations, the dynamic response and seismic retrofit of structures using SPSW systems and LYP steel material have not been studied systematically and adequately, and most of the reported studies have emerged in the recent years.

Considering the importance of assessment of dynamic response as well as seismic retrofit of structures using SPSW systems and LYP steel material, system-level investigations are made via nonlinear time-history analysis of multi-story structures subjected to earthquake ground motions and the results and findings of this study are presented and discussed in this paper.

## 2. Design and properties of structural systems

In order to investigate the seismic retrofit and behavior of structures employing SPSW systems and LYP steel material, a modified version of the 9-story SAC building (FEMA 355C, 2000) designed for seismic and wind conditions in Los Angeles is considered in this study. The floor plan and elevation for the considered and modified Los Angeles 9-story SAC building model are shown in Fig. 1. This building consists of perimeter moment-resisting frames shown by solid lines as the lateral force-resisting system and also interior gravity frames shown by dashed lines. As shown in the figure, in contrast to the original 9-story SAC building, fixed column bases and constant story height are considered in the modified version of this building. In addition, no basement is considered in the building under study.

In order to achieve the objectives of this study and also evaluate the seismic performance of

moment-resisting and SPSW lateral force-resisting systems, two-dimensional numerical models of moment-resisting and gravity-SPSW frames are developed and studied, which represent only the lateral force-resisting system of the building. Furthermore, the *P*-delta effects caused by gravity loads tributary to the interior simple gravity frames are also taken into account. Hence, in addition to consideration of the designed moment-resisting frame, an existing interior gravity frame is retrofitted with steel infill plates applied in the middle bay, as shown in Fig. 1.

The design of the considered 9-story SAC building was based on design practices prevalent before the Northridge earthquake with the standard beam-to-column welded connection details (FEMA 355C, 2000). The sections used in the moment-resisting and gravity frames (pre-Northridge design) are summarized in Table 1. Included in the table are also the designed SPSW horizontal and vertical boundary element, i.e., HBE (beam) and VBE (column), sections and web-plate thicknesses.

The SPSW with conventional steel infill plates has been designed for a site class D (stiff) soil and the adjusted maximum considered earthquake spectral response parameters at 0.2 and 1.0 sec periods,  $S_{MS}$  and  $S_{M1}$ , are 2.415 g and 1.269 g, respectively, where *g* is the acceleration of gravity. Resulting design spectral acceleration parameters at 0.2 and 1.0 sec,  $S_{DS}$  and  $S_{D1}$ , are 1.610 g and 0.846 g, respectively. The equivalent lateral force procedure, per ASCE 7-10 (2010), is used to determine the design seismic loads for the web plates. In design of the SPSW, the conventional steel web plates are assumed to resist the entire story shear demand and the horizontal as well as vertical boundary elements (HBEs and VBEs) are designed using capacity design principles per AISC 341-10 (2010) seismic provisions. The SPSW frame is designed for high-seismic loading and high ductility. ASTM A36 and ASTM A572 Gr. 50 steel material are considered in design of the infill plates and boundary frame elements, respectively. Some key design checks for the

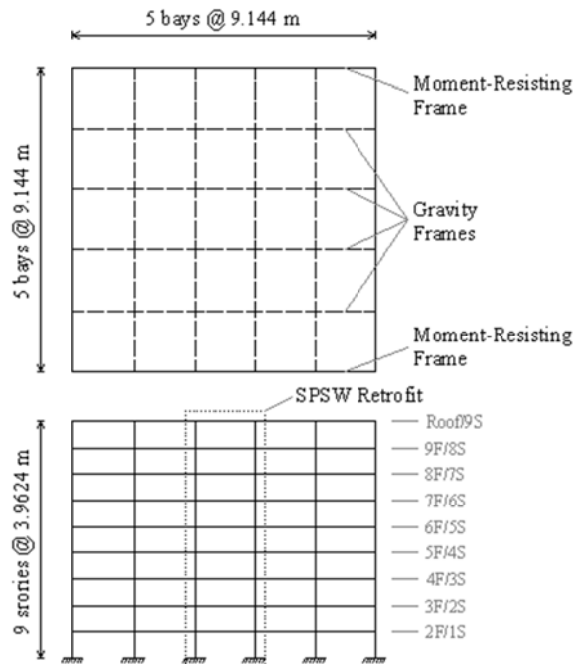


Fig. 1 Floor plan and elevation for the modified LA 9-story SAC building model

Table 1 Properties of the moment-resisting and gravity frames (pre-Northridge design) from the LA 9-story SAC building model and SPSW structure

Story/ Floor	Moment-Resisting Frame			Gravity Frame		SPSW		$t_p$ (mm)
	Girders	Columns		Beams	Columns	HBEs	VBEs	
		Exterior	Interior					
9/Roof	W24×68	W14×233	W14×257	W16×26	W14×48	W30×391	W14×605	1.59
8/9	W27×84	W14×233, W14×257	W14×257, W14×283	W18×35	W14×48, W14×82	W30×391	W14×605	3.18
7/8	W30×99	W14×257	W14×283	W18×35	W14×82	W30×391	W14×665	4.76
6/7	W36×135	W14×257, W14×283	W14×283, W14×370	W18×35	W14×82, W14×109	W30×391	W14×665	6.35
5/6	W36×135	W14×283	W14×370	W18×35	W14×109	W30×391	W14×730	7.94
4/5	W36×135	W14×283, W14×370	W14×370, W14×455	W18×35	W14×109, W14×145	W27×146	W14×730	7.94
3/4	W36×135	W14×370	W14×455	W18×35	W14×145	W30×391	W14×730	9.53
2/3	W36×160	W14×370, W14×370	W14×455, W14×500	W18×35	W14×145, W14×193	W27×146	W14×730	9.53
1/2	W36×160	W14×370	W14×500	W18×35	W14×193	W27×146	W14×730	9.53

Table 2 Some key demand-to-capacity ratios for the SPSW boundary frame elements

Story	Stiffness ( $I_d / I_c$ )		Flexural strength ( $Z_d / Z_c$ )		Combined comp. & flex. (<1.00)	
	HBE	VBE	HBE	VBE	HBE	VBE
9	1.01	0.03	0.33	0.04	0.40	0.71
8	1.01	0.06	0.33	0.09	0.42	0.81
7	1.01	0.08	0.33	0.12	0.43	0.82
6	1.01	0.10	0.33	0.15	0.45	0.98
5	1.01	0.11	0.33	0.17	0.46	1.02
4	0.00	0.11	0.10	0.17	0.78	0.75
3	1.01	0.13	0.33	0.21	0.54	1.13
2	0.00	0.13	0.10	0.21	0.90	1.02
1	0.00	0.13	0.10	0.21	0.90	1.12

boundary frame elements are given in Table 2. In this table,  $I$  is the moment of inertia and  $Z$  is the plastic section modulus.

Eight structural models including moment-resisting frame and retrofitted gravity frame using conventional and LYP steel infill plates are considered in this study, which are listed in Table 3. In the GF-CSPSW model, the steel shear wall is designed by considering conventional steel infill plates as explained before. In the GF-LYPSPSW model series, as shown in Table 3, the conventional steel infill plates of the GF-CSPSW model are replaced by LYP steel plates with increasing thickness, while the same code-designed HBEs and VBEs are used. LYP steel shear walls with increasing web-plate thicknesses are considered in this research in order to address the retrofit of new and existing structures using LYP steel shear wall systems with relatively thicker

plates compared to those with conventional steel plates. It is noted that consideration of LYP steel with considerably lower yield stress will result in relatively thicker plates in design of SPSW systems compared to the application of conventional steel material. Included in Table 3 are also the nominal (expected) base shear ratios ( $V_n/V_{n, GF-CSPSW}$ ) for the considered structural models. Yield stresses of 100 MPa, 250 MPa, and 345 MPa are used for LYP, ASTM A36, and ASTM A572 Gr. 50 steel materials, respectively, in calculation of the nominal base shear strengths.

It should be noted that use of LYP steel enables the design of SPSW systems with web plates having relatively low yielding and high buckling capacities. On this basis, the *limiting* thicknesses of plates corresponding to concurrent geometrical-material bifurcation for the ASTM A36 and LYP100 steel material are estimated in order for evaluating the buckling and yielding behavior of web plates in the SPSW frames. The limiting plate thickness is determined by setting the critical shear stress of a rectangular clamped plate subjected to shear loading equal to the plate shear yield stress determined by considering the von Mises yield criterion. The web-plate slenderness ratios of all stories for the structural models are plotted in Fig. 2. As well, the limiting plate slenderness ratios for respective conventional and LYP steel material are depicted by solid and dashed lines.

Table 3 Considered structural models

Model	Description	Infill plate thickness	Nominal (expected) base shear ratio ( $V_n/V_{n, GF-CSPSW}$ )
MRF	Moment-resisting frame	-	0.78
GF	Gravity frame	-	0.23
GF-CSPSW	Gravity frame with conventional steel plate shear wall	$t_p$	1.00
GF-LYPSPSW1	Gravity frame with replaced LYP steel plate shear wall	$1.0 \times t_p$	0.40
GF-LYPSPSW1.5	Gravity frame with replaced LYP steel plate shear wall	$1.5 \times t_p$	0.60
GF-LYPSPSW2	Gravity frame with replaced LYP steel plate shear wall	$2.0 \times t_p$	0.80
GF-LYPSPSW2.5	Gravity frame with replaced LYP steel plate shear wall	$2.5 \times t_p$	1.00
GF-LYPSPSW3	Gravity frame with replaced LYP steel plate shear wall	$3.0 \times t_p$	1.20

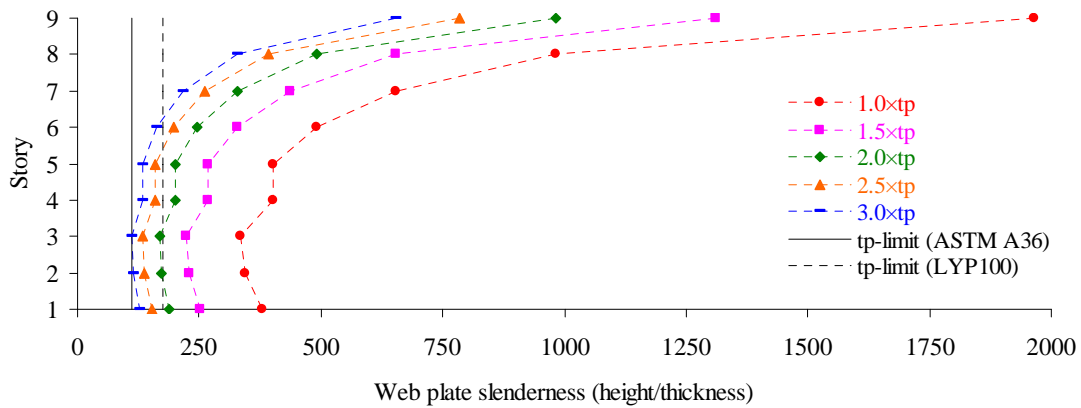


Fig. 2 Evaluation of buckling and yielding behavior of web plates in the structural models

From Fig. 2, it is apparent that consideration of LYP steel results in relatively higher slenderness ratio due to lower limiting plate thickness. This indicates that infill plates of more structural models and stories may primarily undergo yielding before buckling. As seen in the figure, due to larger thickness and lower slenderness of plates at lower stories, these plates can exhibit improved buckling and desirable yielding behaviors. In particular, plates in lower stories of GF-LYPSW3, GF-LYPSW2.5, and GF-LYPSW2 models are expected to undergo early yielding and inelastic buckling. In fact, early yielding of the plate will result in absorption of more seismic energy and consequently decreasing of the overall system demand on the boundary frame members.

### 3. Finite element modeling and verification

Finite element models of the considered structures are developed and analyzed using ANSYS 14.0 (2011) software. The typical bare frame and wall-frame structural models along with the considered finite element mesh scheme are shown in Fig. 3. As discussed before, columns are fully fixed at their bases and the frame beam and column components are assumed to be laterally braced against out-of-plane deformations. Beam-to-column joints are modeled as moment-resisting connections. Also, constraints are used at story level column nodes in order to simulate the effect of a rigid diaphragm.

BEAM188 element is used to model the beam and column components of the frame. This three-dimensional two-node line element with six or seven (warping magnitude) degrees of freedom at each node is suitable for analyzing slender to moderately stubby/thick beam structures and is also well-suited for linear, large rotation, and/or large strain nonlinear applications. Considering the capabilities of this element in handling the associated nonlinear material properties, no strength degrading nonlinear hinges were required to be included for material nonlinearity in the models. In addition, the element is based on Timoshenko beam theory which includes shear-deformation effects, and provides options for unrestrained and restrained warping of cross-sections.

As shown in Fig. 3(b), the strip model approach is used to represent SPSW behavior, and accordingly the web plates are represented by 15 equally-spaced discrete pin-ended and tension-only strips. The angle of inclination of the tension field ( $\alpha$ ) is considered as the strip angle, which

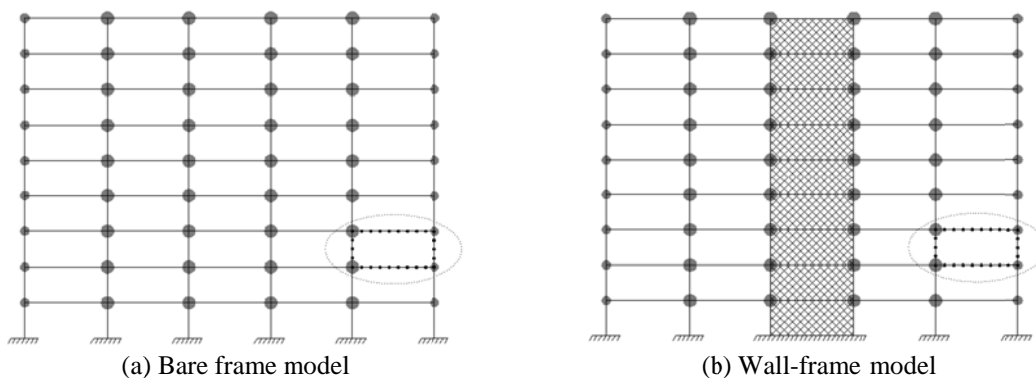


Fig. 3 Bare frame and wall-frame structural models

is taken as  $45^\circ$  in the finite element modeling. The strips are modeled using LINK180 three-dimensional truss element. This element is a uniaxial tension-compression element with three degrees of freedom at each node, which can be used to simulate the tension- and compression-only options, and has plasticity, rotation, large deflection, and large strain capabilities. Strip elements with the selected tension-only option are used in both tension field directions in order for representing the dynamic behavior of the SPSW frames.

Seismic and lumped masses consistent with the FEMA 355C (2000) reported values are placed at each story level on the beam-column intersection nodes, as illustrated in Fig. 3. Lumped masses are modeled using MASS21 point element with up to six degrees of freedom.

ASTM A36 and LYP100 steel material are considered for the infill plates, and ASTM A572 Gr. 50 steel is employed in modeling of the frame beam and column components. The stress-strain curves and mechanical properties of the aforementioned steel material are shown in Fig. 4. The von Mises yield criterion is adopted for material yielding, and kinematic hardening rule is incorporated in the nonlinear time-history analyses.

Rayleigh proportional damping with a damping ratio of 2% is selected and applied in all seismic analyses, which is consistent with the level of damping used in studies on the performance of moment-resisting and SPSW frames by Gupta and Krawinkler (1999) and Berman (2011), respectively. Modal and nonlinear time-history analyses with geometrical and material nonlinearities have been conducted in this study, which are discussed in the subsequent sections.

In order to verify the adequacy of the finite element strip modeling approach in capturing the dynamic behaviors of the structures with various material (yielding) and geometrical (buckling) properties, finite element results are validated through comparison with different published experimental results. To achieve this, single- and multi-story reference SPSWs with slender (buckling before yielding) and stocky (yielding before buckling) infill plates employing conventional and LYP steel material have been considered. Modeling details and comparison results are provided in Fig. 5.

Fig. 5(a) shows the modeling details and comparison results for the one-story one-bay SPSW2 specimen employing slender and conventional steel infill plate tested by Lubell (1997). The modeling details and comparison results for Chen and Jhang's (2006) specimen no. 1 with stocky and LYP100 steel infill plate are illustrated in Fig. 5(b). As shown, the RBS connections are properly considered in finite element modeling in this case. In addition to the results of the two single-story SPSW test specimens, the strip modeling details and verification results for the three-

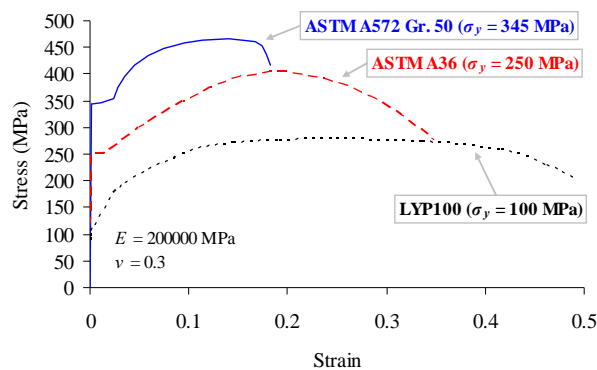
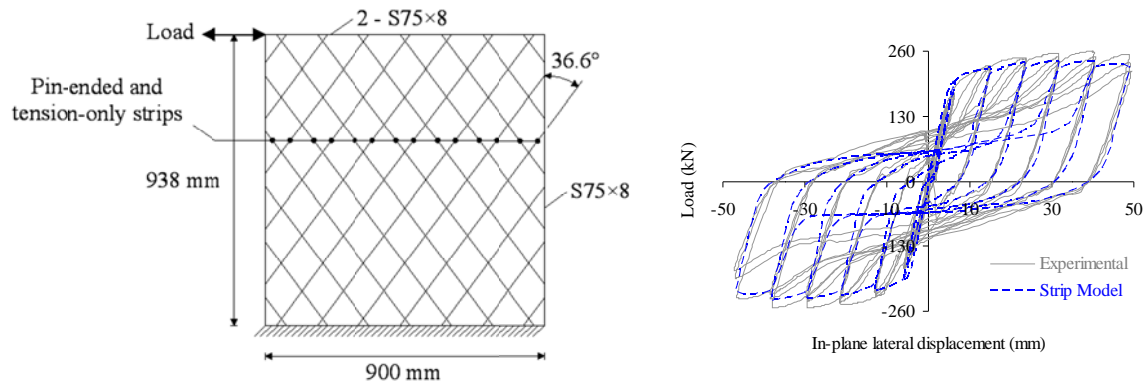
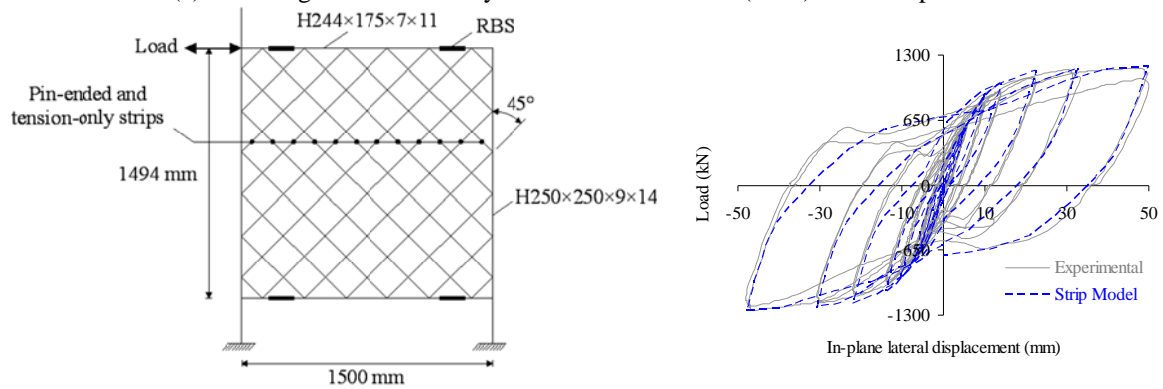


Fig. 4 Material properties of the steel used



(a) Modeling details and analysis results for Lubell's (1997) SPSW2 specimen



(b) Modeling details and analysis results for Chen and Jhang's (2006) specimen no. 1

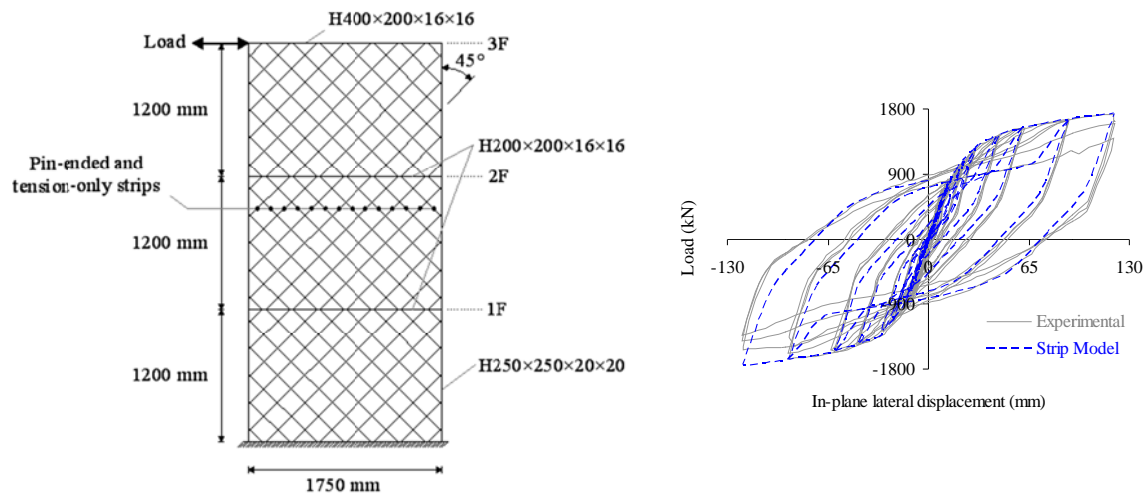
(c) Modeling details and analysis results (3F) for Park *et al.*'s (2007) SC2T specimen

Fig. 5 Validation of SPSW finite element strip modeling

story SC2T specimen with thin infill plates and strong columns tested by Park *et al.* (2007) are also shown in Fig. 5(c). The infill plates and frame members of the SC2T specimen were made of

SS400 and SM490 steel material (Korean Standard) with 240 and 330 MPa yield stresses, respectively. From the figures, it is quite evident that the predictions of the strip model agree well with the test results. These findings indicate that the applied strip model, using ANSYS 14.0 (2011) software, is quite capable of predicting the response of single- and multi-story SPSWs with various geometrical (buckling) and material (yielding) properties.

#### 4. Modal analysis and elastic behavior

Modal analyses are performed to determine the vibration characteristics including natural frequencies as well as mode shapes, and initial stiffnesses of the structural models. Fig. 6, for instance, shows the first three mode shapes of vibration obtained from modal analysis of the GF-CSPSW model.

Accurate determination of vibration characteristics, in particular, the fundamental period of vibration is of great importance in calculating the lateral forces and seismic design of a structure. Most building codes propose simple empirical expressions to evaluate the fundamental period of vibration. According to ASCE 7-10 (2010), the approximate fundamental period ( $T_a$ ), in seconds, can be determined from the following equation

$$T_a = C_t h_n^x \quad (1)$$

in which,  $h_n$  is the height of the structure above the base,  $C_t=0.0724$  and  $x=0.8$  for steel moment-resisting frames, and  $C_t=0.0488$  and  $x=0.75$  for other structural systems including SPSWs. The accuracy of the code predictions for the fundamental periods of SPSW systems has been evaluated through numerical analyses by Topkaya and Kurban (2009), Berman (2011), Bhowmick *et al.* (2011). These studies have demonstrated that, in general, the code-specified formulae fail in providing accurate estimates for the fundamental periods of SPSWs, and accordingly simple and relatively accurate methods and formulae have been proposed by Topkaya and Kurban (2009) and Bhowmick *et al.* (2011) for predicting the fundamental period of SPSW systems. In this study, the periods of the considered structural models are determined from the modal analyses and tabulated in Table 4. These numerical estimates are compared with the corresponding period values reported in FEMA 355C (2000) and predicted by the ASCE 7-10 (2010) specified equation, i.e., Eq. (1), in Table 4.

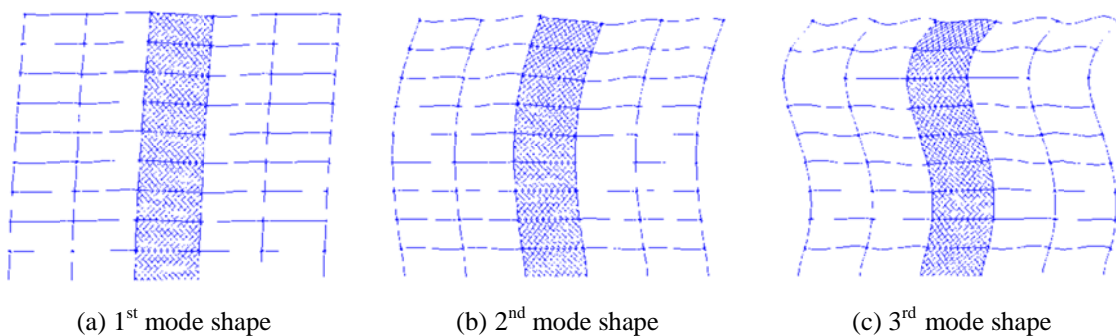


Fig. 6 Mode shapes of the GF-CSPSW model

Table 4 Periods of the considered structural models

Model	$T_{Analysis}$ (sec)	$T_{SAC}$ (sec)	$T_{ASCE}$ (sec)	$T_{Analysis}/T_{ASCE}$
MRF	$T_1=2.097$	$T_1=2.34$	1.264	1.66
	$T_2=0.789$	$T_2=0.88$	-	-
	$T_3=0.456$	$T_3=0.50$	-	-
GF-CSPSW	$T_1=1.036$	-	0.711	1.46
GF-LYSPSW1	$T_1=1.036$	-	0.711	1.46
GF-LYSPSW1.5	$T_1=0.976$	-	0.711	1.37
GF-LYSPSW2	$T_1=0.944$	-	0.711	1.33
GF-LYSPSW2.5	$T_1=0.923$	-	0.711	1.30
GF-LYSPSW3	$T_1=0.909$	-	0.711	1.28

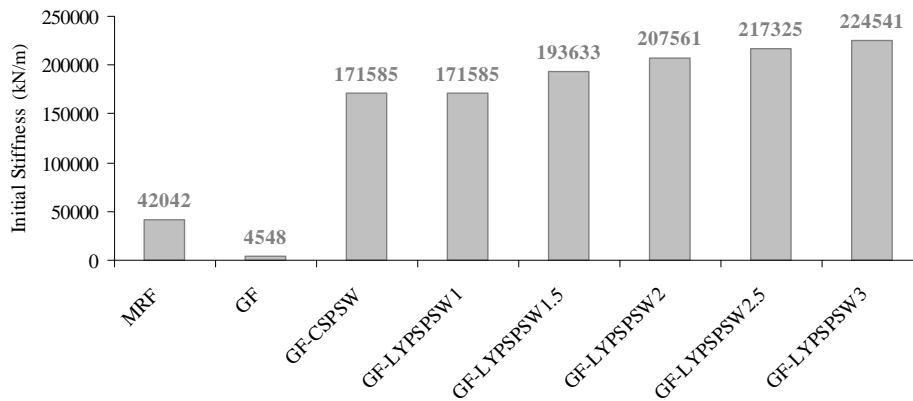


Fig. 7 Initial stiffnesses of the considered structural models

As seen in the table, in spite of the modifications made in the original 9-story SAC building, the first three periods of the considered MRF model obtained from the modal analysis are found to be in good agreement with the values reported in FEMA 355C (2000). Nevertheless, the two values of the fundamental period for this structural system, i.e.,  $T_{1,Analysis}$  and  $T_{1,SAC}$ , are considerably larger than that predicted by Eq. (1).

Table 4, also, shows that Eq. (1) specified by the ASCE 7-10 (2010) code provides a constant value for the fundamental periods of SPSWs with increasing infill plate thicknesses, while the fundamental periods obtained from modal analyses exhibit a decreasing trend, as expected, due to the increase in stiffness. In addition, consistent with the results of the aforementioned studies on the periods of SPSW systems, ASCE 7-10 (2010) code-specified equation, i.e., Eq. (1), is found to yield lower estimates for the fundamental periods of SPSW systems compared to numerical predictions. This discrepancy diminishes slightly as the infill plate thickness increases and the system gains more stiffness.

The values of initial stiffness of the considered structural models determined from the modal analyses are shown in Fig. 7. As seen in the figure, the GF model possesses a very low initial stiffness, and also the GF-SPSW models in general exhibit a considerably higher initial stiffness compared to the MRF model. It is also evident that the initial stiffness of a GF-LYSPSW model

increases due to the increase in the infill plate thickness.

These results indicate that GF-CSPSW model possesses much higher initial stiffness and lower fundamental period compared to the MRF model. Furthermore, retrofit of the GF-CSPSW model with thicker and LYP steel infill plates results in increasing of the initial stiffness by maximum 30% and decreasing of the fundamental period by maximum 10% approximately in the extreme considered case, i.e., GF-LYPSW3 model. In spite of the fact that higher initial stiffness can effectively control the drift and damages to the structural system and drift-sensitive nonstructural components, it may make the structure shake at higher acceleration levels and more damage may be expected to acceleration-sensitive nonstructural components and contents (HAZUS-MH MR5, 2010). Therefore, evaluation of seismic performance and level of induced floor accelerations due to ground motion excitations is essential in efficient seismic design and retrofit of structures.

Lastly, modal analysis results have been utilized to determine the Rayleigh damping coefficients, i.e., the mass and stiffness matrix multipliers, by considering the 1<sup>st</sup> and 5<sup>th</sup> modal frequencies in order to set the damping ratio at 2%. In other words, the mass and stiffness matrix multipliers are determined by using  $2\zeta\omega_1\omega_5/(\omega_1 + \omega_5)$  and  $2\zeta/(\omega_1 + \omega_5)$  equations, respectively, where  $\zeta$  is the damping ratio (2%) and  $\omega_1$ ,  $\omega_5$  are the respective first and fifth modal frequencies. In addition, the first and fifth modes are selected to ensure reasonable values for the damping ratios in all the modes contributing significantly to the response.

## 5. Nonlinear time-history analysis and selection of ground motions

In order to evaluate the seismic drifts, accelerations, and other behavioral characteristics, nonlinear time-history dynamic analyses are performed for the structural models considered in this study. In order to account for the *P*-delta effects on the seismic response, gravity loads are initially applied on the two-dimensional structural models prior to the time-history dynamic analysis, and then these loads are kept constant while ground accelerations are applied to the base of the structure.

Table 5 Details of selected LA ground motions for seismic performance evaluation

SAC Name	Record	Earthquake magnitude	Distance (km)	Scale factor	PGV (mm/s)	PGA (mm/s <sup>2</sup> )	Probability of exceedance
LA02	Imperial Valley, El Centro, 1940	6.9	10	2.01	599.0	6628.8	10% in 50 years
LA06	Imperial Valley, Array #06, 1979	6.5	1.2	0.84	474.4	2300.8	10% in 50 years
LA11	Loma Prieta, Gilroy, 1989	7	12	1.79	791.4	6524.9	10% in 50 years
LA16	Northridge, Rinaldi RS, 1994	6.7	7.5	0.79	1007.6	5685.8	10% in 50 years
LA18	Northridge, Sylmar, 1994	6.7	6.4	0.99	1189.3	8014.4	10% in 50 years
LA19	North Palm Springs, 1986	6	6.7	2.97	682.7	9994.3	10% in 50 years
LA21	Kobe, 1995	6.9	3.4	1.15	1427.0	12580.0	2% in 50 years
LA23	Loma Prieta, 1989	7	3.5	0.82	737.6	4099.5	2% in 50 years
LA25	Northridge, Rinaldi, 1994	6.7	7.5	1.29	1603.1	8516.2	2% in 50 years
LA28	Northridge, Sylmar, 1994	6.7	6.4	1.61	1935.3	13041.0	2% in 50 years
LA29	Tabas, 1974	7.4	1.2	1.08	710.5	7934.5	2% in 50 years

A total of eleven earthquake acceleration time histories are selected from the Los Angeles ground motions developed for the SAC steel research project (FEMA 355C, 2000) for the time-history response analysis. Details of the selected earthquake records including the magnitude, distance, scale factor, peak ground velocity (PGV), peak ground acceleration (PGA), and hazard level are given in Table 5.

Time-history acceleration records are selected in a manner to cover earthquakes with minimum, average, and maximum PGV and PGA values within both 10/50 (10% probability of exceedance in 50 years) and 2/50 (2% probability of exceedance in 50 years) hazard levels. Hence, the selected ground motions will enable the seismic behavior to be studied at 10/50 and 2/50 seismic hazard levels that represent design and maximum earthquakes. The selected earthquake records have PGA values ranging between 0.23 g and 1.33 g. The results of the nonlinear time-history dynamic analyses are discussed in the following sections.

## 6. Nonlinear time-history analysis results

### 6.1 Story and interstory drift ratios

Lateral displacement (drift) is one of the important parameters in design of structures, and structures should be designed to accommodate the displacements imposed by lateral forces since excessive drift may constitute unacceptable performance. Among the lateral force-resisting systems, SPSWs are deemed to be highly-efficient systems which can be considered for many retrofit applications and are very effective in controlling drift. According to Seilie and Hooper (2005), SPSW systems are capable of surviving up to 4% drift ratio. Similar conclusion may be drawn from the study reported by Baldvins *et al.* (2012). LYP steel shear walls, in particular, have been shown to reach even larger drift ratios up to 5-6% through stable deformation. Despite these findings, widespread use of SPSW systems particularly with LYP steel infill plates requires further investigation of various design and performance aspects.

As part of the dynamic response assessment, *story* and *interstory* drift ratios of the considered structural models induced by seismic excitations are evaluated in this section. It is noted that *story* drift ratio is the horizontal deflection at the top of the story relative to the base of the structure divided by the height above the base to the same level, while *interstory* drift ratio is the horizontal deflection at the top of the story relative to the bottom of the story divided by the story height. The average story and interstory drift ratios of the lateral force-resisting systems obtained by considering the maximum story responses for all ground motions are shown in Fig. 8.

From Figs. 8(a)-(b), it is apparent that the values of the interstory drift ratio are relatively larger than those of the story drift ratio. These results indicate that the interstory drift ratio parameter is more critical and controlling than the story drift ratio parameter in seismic design of structures. Moreover, as seen in the figures, the story and interstory drift ratios of all structures are less than the prescribed 2.0% limit, except for the interstory drift ratios of the MRF model which exceed the 2.0% limit at some stories. It is also found that the code-designed GF-CSPSW model has been quite effective in reducing the drifts compared the MRF model. In addition, retrofitting of the GF-CSPSW model with LYP steel infill plates of the same thickness has unfavorably resulted in larger drift ratios, while consideration of thicker LYP steel infill plates for retrofit purposes has yielded desirable results in limiting the drift ratios.

Variations of the seismic-induced peak story and interstory drift ratios as a result of retrofit of

structures using SPSW systems and LYP steel material are shown in Fig. 9. These average values for the peak drift ratios are obtained by considering the peak drift responses for all ground motions.

These results demonstrate that the peak interstory drift ratios are larger than the peak story drift ratios in all cases which is, in turn, indicative of importance of the interstory drift ratio as an effective design criterion. From the figure, it is evident that the peak interstory drift ratio for the MRF model is close to 3.0% and for the GF-CSPSW model is slightly larger than 2.0%, while SPSW systems retrofitted with LYP steel infill plates have been effective at limiting the peak drift ratios to less than 2.0%. One important finding which requires attention is the slight increase in the peak story and interstory drift ratios in case of the GF-LYPSPSW3 model in spite of the decreasing trend in the peak drift ratios due to the increase in thicknesses of the LYP steel infill plates. Based on the results of the studies reported by Caccese *et al.* (1993) and Habashi and Alinia (2010), the increase in peak drift ratios in this case may be attributed to the fact that large plate thicknesses increase the overall system demand on the adjacent frame particularly vertical boundary members and the performance and failure of the structure may be governed by the column instability.

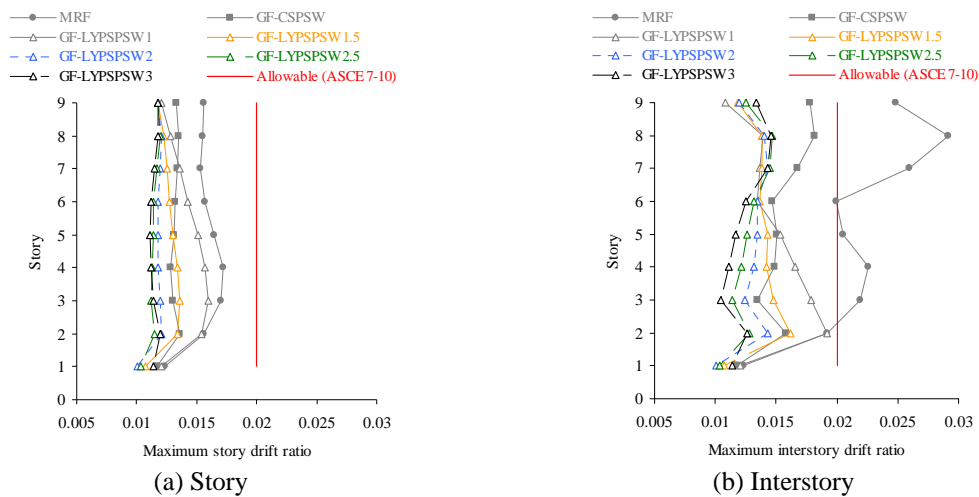


Fig. 8 Maximum story and interstory drift ratios induced by the considered ground motions

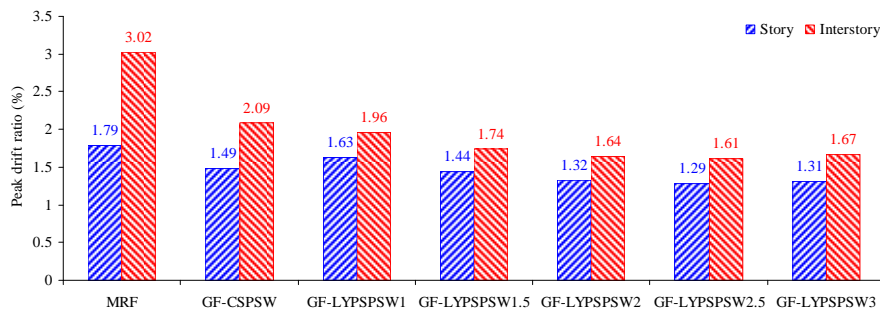


Fig. 9 Variations of seismic-induced peak story and interstory drift ratios due to retrofit of structures using SPSW systems and LYP steel material

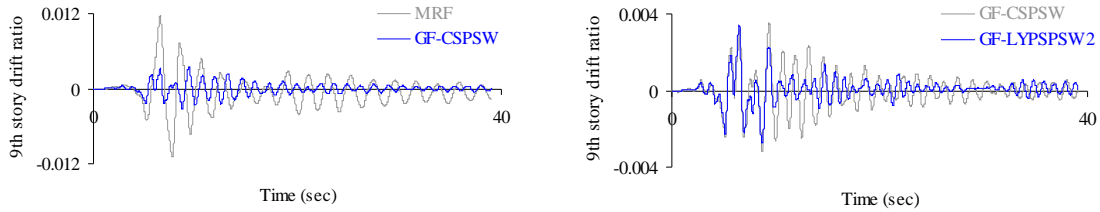


Fig. 10 Comparison of 9<sup>th</sup> story drift ratio time histories of MRF, GF-CSPSW, and GF-LYSPSW2 models

As an example, the 9<sup>th</sup> story drift ratio time histories of the MRF, GF-CSPSW, and GF-LYSPSW2 models for the LA06 ground motion (see Table 5) are shown in Fig. 10, in which the effectiveness of the GF-CSPSW model relative to the MRF model in limiting the 9<sup>th</sup> story drift is demonstrated. Also, this figure shows that retrofit of the GF-CSPSW model with LYP steel infill plates of double thickness, i.e., GF-LYSPSW2 model, results in a desirable drift performance as the 9<sup>th</sup> story drift is effectively decreased due to such a retrofitting strategy.

## 6.2 Story acceleration

Acceleration is another important criterion in seismic design and retrofit of structures which may cause damages to the structural and especially nonstructural systems as well as contents and consequently result in considerable economic loss. While damage to the structural system is the most important measure of building damage affecting casualties and catastrophic loss of function, damage to nonstructural systems and contents tends to dominate economic loss (HAZUS-MH MR5, 2010).

Considering the relatively high stiffness of SPSW systems and its effectiveness in controlling the lateral displacements, the seismic-induced accelerations also have to be taken into consideration in efficient seismic design and retrofit of buildings using such lateral force-resisting systems. In fact, high stiffness may result in elastic behavior of SPSW systems and amplify the acceleration response of the structures. If the SPSW infill plate thicknesses, boundary frame members, and configuration are properly designed to meet the seismic provisions without significant design over-strength, then nonlinearities in the seismic response will reduce expected accelerations (Eatherton 2006).

On this basis, the acceleration responses of the designed and retrofitted structural systems are evaluated in this study. The average story accelerations of the structural models obtained by considering the maximum story responses for all ground motions are shown in Fig. 11.

As seen in the figure, the GF model experienced story accelerations of less than 0.70 g due to its relative flexibility, while the GF-CSPSW model exhibits the largest story acceleration response ranging between 1.32 g and 1.66 g. In addition, as shown, increasing of the infill plate thickness in the GF-LYSPSW models increases the story accelerations. However, it is notable that retrofit of the GF-CSPSW model with LYP steel infill plates of even larger thicknesses still results in relatively smaller seismic-induced story accelerations. This is indeed due to the exclusive material properties of the LYP steel material which results in early plate yielding and desirable nonlinear seismic response of the structure.

The variations of the seismic-induced peak floor accelerations as a result of retrofit of structures using SPSW systems and LYP steel material are illustrated in Fig. 12. The depicted

average values for the peak floor acceleration are obtained by considering the peak acceleration responses for all ground motions.

These results indicate that employment of LYP steel material in design and retrofit of structures in areas with high seismicity would result in desirable seismic performance with limited earthquake-induced peak floor accelerations. From the figure, it is evident that employment of conventional steel infill plates significantly amplifies the peak floor acceleration of the GF-CSPSW model relative to that of the MRF model, whereas retrofitting of the GF-CSPSW model with LYP steel infill plates effectively controls the seismic-induced peak floor acceleration. Even in the extreme case, i.e., GF-LYPSPSW3 model with the largest infill plate thickness, the peak floor acceleration is still below that of the GF-CSPSW model.

The 9<sup>th</sup> story acceleration time histories of the MRF, GF-CSPSW, and GF-LYPSPSW2 models for the sample ground motion LA16 (see Table 5) are shown in Fig. 13. These results show that use of LYP steel infill plates of double thickness in retrofit of the GF-CSPSW model improves the seismic behavior of the structural system by limiting the acceleration response in a quite desirable and efficient manner.

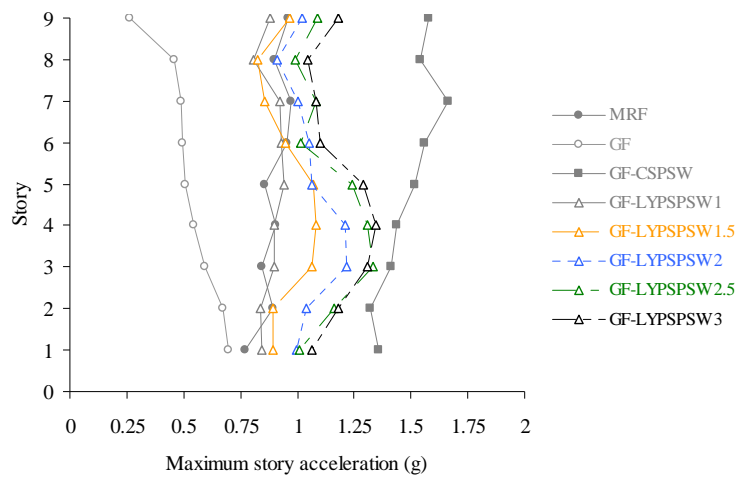


Fig. 11 Maximum story accelerations induced by the considered ground motions

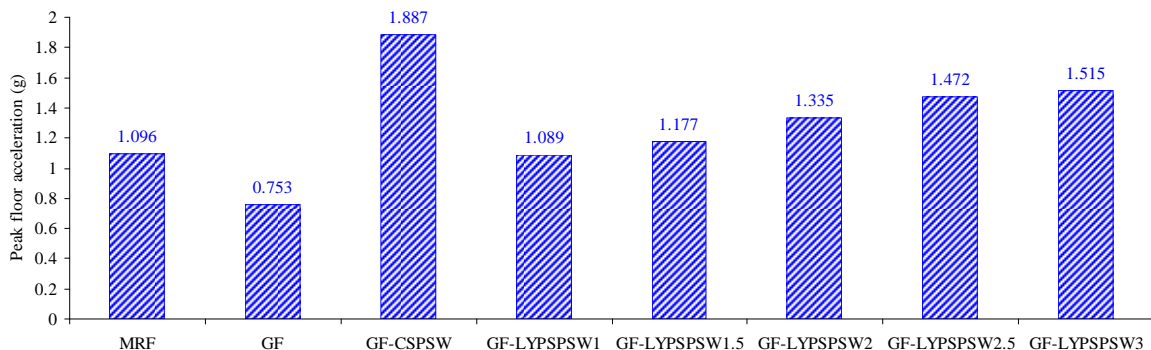


Fig. 12 Variations of seismic-induced peak floor accelerations due to retrofit of structures using SPSW systems and LYP steel material

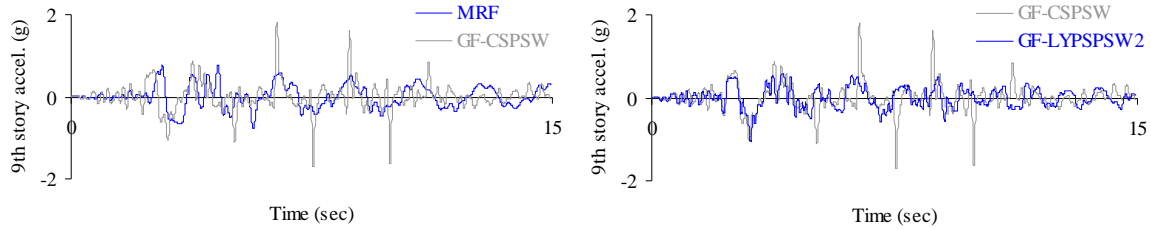


Fig. 13 Comparison of 9<sup>th</sup> story acceleration time histories of MRF, GF-CSPSW, and GF-LYSPSW2 models

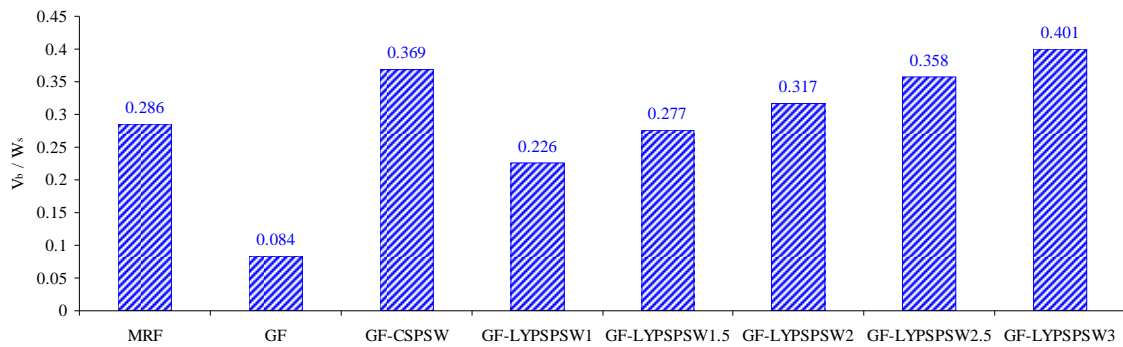


Fig. 14 Variations of seismic-induced normalized maximum base shear demands due to retrofit of structures using SPSW systems and LYP steel material

### 6.3 Base shear

The seismic-induced base shear demands of the structural models are evaluated in this section. The base shear demands ( $V_b$ ) are obtained from the nonlinear time-history dynamic analyses and normalized with the seismic weight ( $W_s$ ) of the structure. Fig. 14 shows the variations of the seismic-induced normalized maximum base shear demands due to the retrofit of structures using SPSW systems and LYP steel material. The average  $V_b/W_s$  values shown in the figure are obtained by considering the  $V_b/W_s$  values for all ground motions.

As shown in Fig. 14, the base shear demand of the GF-CSPSW model is larger than that of the MRF model. Retrofit of the GF-CSPSW model with LYP steel infill plates of the same or slightly larger thicknesses, on the other hand, significantly reduces the base shear demand of the SPSW system. However, use of thicker plates, particularly in GF-LYSPSW2.5 and GF-LYSPSW3 models, increases the base shear absorbed by the SPSW system and unfavorably results in relatively large base shear demands. These results indeed demonstrate that application of LYP steel infill plates of double thickness is apparently the optimal choice in retrofitting of the conventional steel and code-designed GF-CSPSW model.

The base shear time-history plots of MRF, GF-CSPSW, and GF-LYSPSW2 models for the LA23 ground motion (see Table 5), for instance, are provided in Fig. 15. From the figure, it is evident that application of LYP steel infill plates of double thickness results in reduced seismic-induced base shear demands in addition to its advantages in improving the stiffness, and buckling as well as energy absorption capacities of the system.

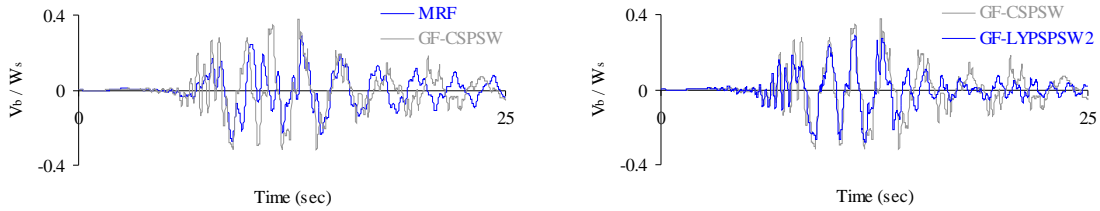


Fig. 15 Comparison of base shear time histories of MRF, GF-CSPSW, and GF-LYPSPSW2 models

### 6.4 Base moment

This section deals with the assessment of the base moment demands of the structural models which are estimated by summing the moments developed at column bases due to seismic loading. Base moments ( $M_b$ ) have been normalized by the product of the seismic weight ( $W_s$ ) and total height of the structure ( $H_t$ ). Shown in Fig. 16 are the variations of the seismic-induced normalized maximum base moment demands due to the retrofit of structures using SPSW systems and LYP steel material. The illustrated average  $M_b/(W_s \times H_t) \times 100$  values are obtained by considering the corresponding values for all ground motions.

Fig. 16 shows that the GF-CSPSW model possesses remarkably lower base moment demand compared to the MRF model, and use of LYP steel infill plates with increasing thickness further reduces the base moment demand. However, from the figure it is apparent that the base moment demand increases slightly in case of the GF-LYPSPSW3 model with the thickest infill plates.

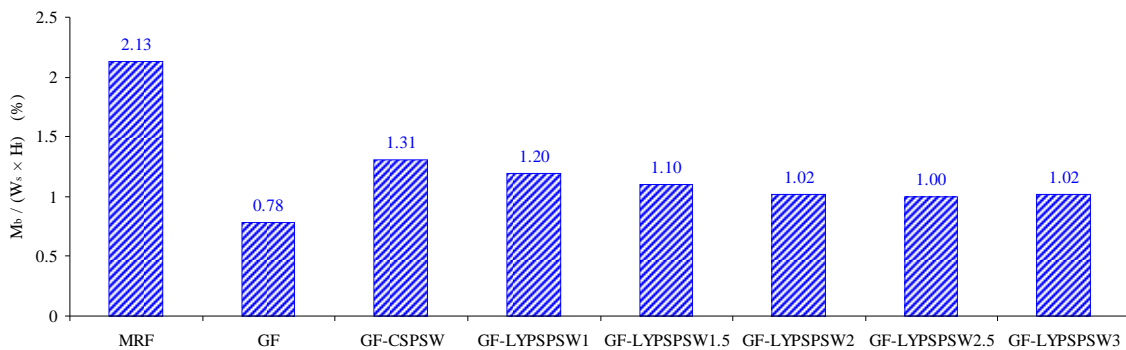


Fig. 16 Variations of seismic-induced normalized maximum base moment demands due to retrofit of structures using SPSW systems and LYP steel material

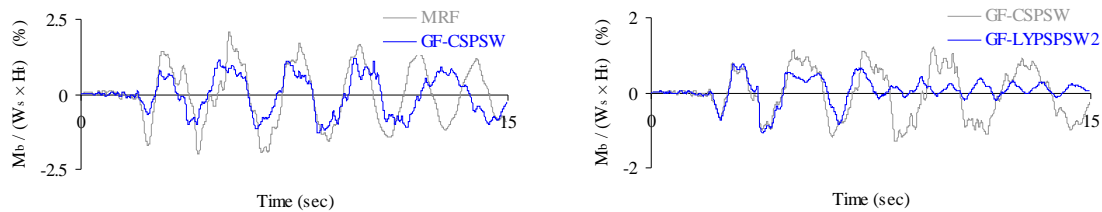


Fig. 17 Comparison of base moment time histories of MRF, GF-CSPSW, and GF-LYPSPSW2 models

The base moment time-history plots of MRF, GF-CSPSW, and GF-LYPSPSW2 models for the LA16 ground motion (see Table 5), as an example, are shown in Fig. 17. These plots confirm that the base moment demand of the GF-CSPSW model is lower than that of the MRF model. Also, employment of LYP steel infill plates with double thickness in the GF-LYPSPSW2 model effectively reduces the base moment demand in comparison with the response of the GF-CSPSW model.

### 6.5 VBE axial loads at column bases

According to the fundamental mechanics of SPSWs, VBES are subjected to combined axial force and transverse force developed by the tension-field action of the infill plates. Therefore, changes in web-plate thickness as well as material properties can have a significant impact on the design and performance of the surrounding column members in such systems. On this basis, the effects of retrofitting of SPSW systems with LYP steel infill plates of relatively larger thicknesses on the VBE axial load demands are evaluated in this section. The maximum VBE axial loads at the column bases ( $P_{VBE-base}$ ) have been normalized by the axial yield strength ( $P_y$ ) of the first story VBE, i.e., W14×730 (see Table 1). The average  $P_{VBE-base}/P_y$  values obtained from the normalized maximum VBE axial load demands at column bases for all ground motions are shown in Fig. 18.

Fig. 18 shows that increasing of the infill plate thickness increases the VBE axial load demand. Also, retrofit of the GF-CSPSW model using LYP steel infill plates with 1.0, 1.5, and 2.0 times (larger) thicknesses results in relatively smaller VBE axial load demands, while the GF-LYPSPSW2.5 and GF-LYPSPSW3 models possess larger VBE axial load demands compared to the GF-CSPSW model. This finding demonstrates that the GF-LYPSPSW2 model can be a desirable retrofit option for the GF-CSPSW model, which is consistent with the other findings of this study. It is important to note that such a favorable seismic response is provided as a result of influence of the advantageous LYP steel material properties.

### 6.6 Web plate ductility ratio and energy dissipation mechanism

Structural systems designed for high-seismic loading are expected to undergo multiple cycles of loading into the inelastic range with controlled damage accepted as a means of dissipating the

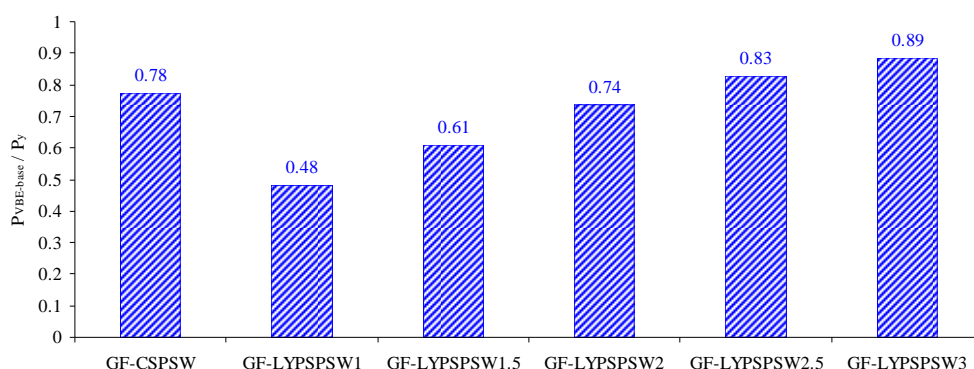


Fig. 18 Variations of seismic-induced normalized maximum VBE axial load demands at column bases due to retrofit of SPSWs using LYP steel material

energy of the earthquake. The ability of a system to withstand such loading is termed *system ductility*. In the case of SPSW systems, the web plates are the locations where inelastic strain demands are primarily expected to occur, and hence ductility of steel web plates in such lateral force-resisting systems will result in good performance under severe seismic loading. On this basis, the high-seismic design of SPSW systems is based on confining ductility demands primarily to the web plates and also to plastic hinges in the HBE at the VBE face (Sabelli and Bruneau 2006).

Based on the reported studies on SPSWs, as partly listed by Sabelli and Bruneau (2006), properly-designed systems have by and large exhibited significant ductility. For instance, some conventional and LYP steel shear walls tested by Berman and Bruneau (2005) and Chen and Jhang (2006, 2011), respectively, reached a web plate ductility ratio of 12 prior to failure.

In this section, the web plate ductility demands for all stories of the GF-CSPSW and GF-LYPSWS2 models are determined from nonlinear time-history analyses and evaluated comparatively in order to further verify the effectiveness of the conventional steel shear wall retrofit strategy using LYP steel infill plates with double thicknesses. The average values of the maximum web plate ductility ratio for all stories of the two considered models are shown in Fig. 19. These values are obtained from the maximum web plate ductility ratios for all stories of the two models and also all considered ground motions. The maximum ductility ratio for each story is determined from the maximum plastic strain of a strip element with the largest maximum plastic strain value divided by the yield strain.

From the figure, it is found that the web plate ductility ratios for all stories of the two models lie between 4 and 6.5. Also, it is evident that the story ductility ratios of the GF-LYPSWS2 model are in general larger than those of the GF-CSPSW model except for the upper stories, in particular the 9<sup>th</sup> story, where GF-CSPSW web plates exhibit relatively larger ductility ratio. These results demonstrate that ductility performance of the GF-CSPSW and GF-LYPSWS2 models is by and large similar and even application of LYP steel in GF-LYPSWS2 model with thicker infill

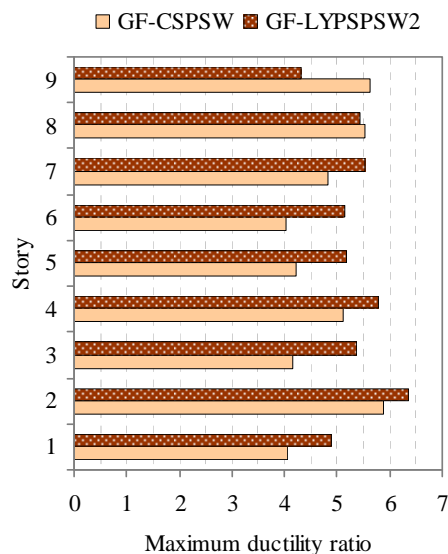
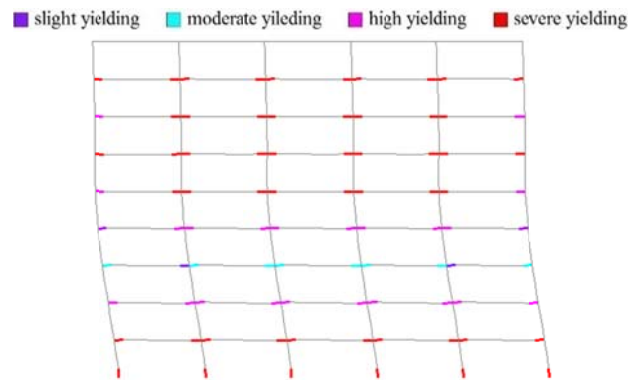
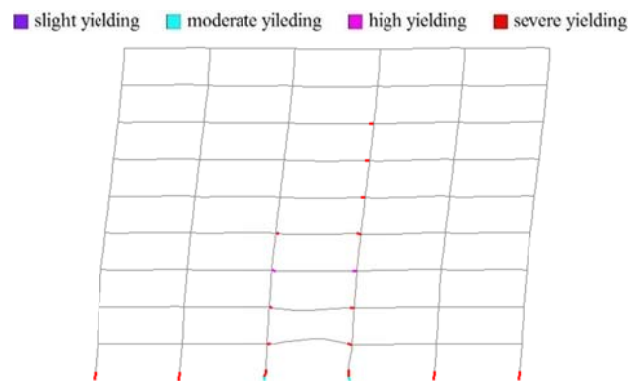


Fig. 19 Average web plate ductility ratios of GF-CSPSW and GF-LYPSWS2 models

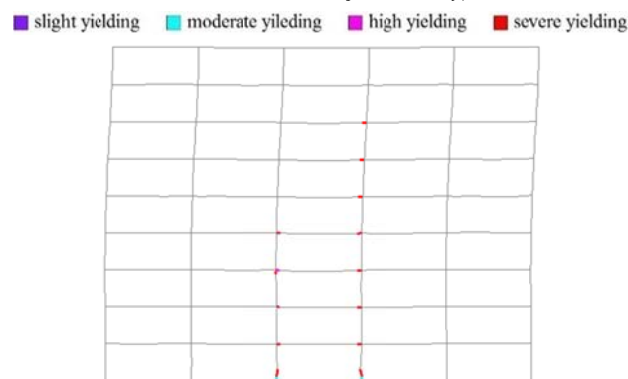
plates results in relatively larger ductility and desirable energy dissipation mechanism of the system in which most of the earthquake energy is dissipated through inelastic deformations developed in the web-plate components.



(a) MRF



(b) GF-CSPSW (frame only)



(c) GF-LYPSPSW2 (frame only)

Fig. 20 Strain energy contour plots for MRF, GF-CSPSW (frame only), and GF-LYPSPSW2 (frame only) models at the end of application of LA28 ground motion showing the plastification zones in beam/HBE and column/VBE frame members

Fig. 20 shows the strain energy contour plots for MRF, GF-CSPSW (frame only), and GF-LYPSWSW2 (frame only) models at the end of application of LA28 ground motion (see Table 5), for instance. This figure intends to show the plastification zones in frame members through which the earthquake energy is partly dissipated in addition to the inelastic deformations in web-plate components in SPSW systems.

Fig. 20(a) shows that in the MRF model the seismic energy is fully dissipated through development of plastic hinges at the ends of beam members and all 1<sup>st</sup> story column bases. Fig. 20(b), on the other hand, shows that in the GF-CSPSW model plastic hinges are formed at the ends of HBEs and all 1<sup>st</sup> story VBE and column bases, while from Fig. 20(c) it is found that the plastic hinges are desirably confined to HBE ends and 1<sup>st</sup> story VBE bases. Consistent results are obtained in cases of other earthquake ground motions; however, the results of only LA28 ground motion are presented in here for brevity. These findings indicate that the code-designed GF-CSPSW model has provided inelastic deformation capacity primarily through web plate yielding and also plastic-hinge formation in the ends of HBEs, as expected. However, the GF-LYPSWSW2 model has apparently exhibited a more favorable behavior by even confining the column-base plastic hinges to the 1<sup>st</sup> story VBE bases and reducing the overall system demand on the frame column members outside the SPSW.

## 7. Conclusions

In this paper, the seismic behavior of code-designed and retrofitted lateral force-resisting systems including 9-story moment-resisting and SPSW frames has been investigated using nonlinear time-history analysis of a suite of structural models under eleven earthquake acceleration time histories with wide ranges of PGV and PGA values within 10/50 and 2/50 hazard levels. The SPSWs were modeled using the strip model which was shown to adequately represent the behavior of single- and multi-story SPSWs with different geometrical-material bifurcation characteristics.

Fundamental periods obtained from the ASCE 7-10 (2010) code-specified formula were found to be lower than those obtained from modal analysis of the moment-resisting and SPSW frames. Such lower estimates of the fundamental period may lead to conservative estimates of the design seismic forces. Based on the modal analysis results, the considered SPSW-frame models possessed remarkably higher initial stiffness and lower period values compared to the MRF model. Moreover, retrofitting of the GF-CSPSW model in the extreme case, i.e., with LYP steel infill plates of triple thickness, resulted in maximum 30% increase in initial stiffness and 10% decrease in the fundamental period values approximately.

Results of the nonlinear time-history analyses showed that *interstory* drift ratio parameter is more controlling and of further significance relative to *story* drift ratio parameter in seismic design of structures. The SPSW systems were found to be quite effective in limiting the drifts of the structural models, and LYP steel shear walls, in particular, exhibited good performance in improving the drift response of the structures. Acceleration response assessment of the code-designed and retrofitted structural models revealed that employment of LYP steel infill plates with even larger thicknesses in retrofitting of the GF-CSPSW model results in relatively smaller floor accelerations. The LYP steel shear wall frames, also, showed a good performance in reducing the base shear and moment demands compared to the GF-CSPSW model. Furthermore, retrofit of the conventional steel SPSW using LYP steel infill plates was found to be effective in lowering the VBE axial load demands at column bases as the web-plate thicknesses increased up to a certain

limit. Consistent with all case studies, it was found that employment of overly thick LYP steel infill plates in retrofit of the GF-CSPSW model may adversely affect the seismic response and result in weak or undesirable performance of the SPSW system.

In a comparative case study, it was also shown that the GF-LYPSPSW2 model possesses relatively larger ductility and energy dissipation capability compared to the GF-CSPSW model. All in all, evaluation of different seismic response parameters demonstrates that the GF-LYPSPSW2 model with LYP steel web-plates of double thickness seems to be a desirable retrofit option for the code-designed and conventional steel GF-CSPSW model.

Lastly, the effectiveness of use of LYP steel with superior material properties compared to conventional steel in improving the seismic performance through either design of new or retrofit of existing structures is demonstrated through system-level investigations presented in this paper. The results and findings of this study are indicative of various advantages of use of LYP steel material in efficient seismic design and retrofit of structures.

## Acknowledgments

The authors would like to express their sincere and profound appreciations to Prof. Carlos Estuardo Ventura from The University of British Columbia in Canada, Prof. Sheng-Jin Chen from National Taiwan University of Science and Technology in Taiwan, Dr. Chyuan Jhang from the Sinotech Engineering Consultants in Taiwan, and Dr. In-Rak Choi from the Research Institute of Industrial Science and Technology in South Korea, for their great support in providing experimental data and details.

## References

- AISC 341-10 (2010), Seismic Provisions for Structural Steel Buildings, American Institute of Steel Construction, Chicago, IL.
- ANSYS 14.0 (2011), ANSYS 14.0 documentation, ANSYS Inc.
- ASCE 7-10 (2010), Minimum Design Loads for Buildings and Other Structures, American Society of Civil Engineers, Reston, VA.
- Baldvins, N.M., Berman, J.W., Lowes, L.N., Janes, T.M. and Low, N.A. (2012), "Fragility functions for steel plate shear walls", *Earthq. Spectra*, **28**(2), 405-426.
- Berman, J.W. (2011), "Seismic behavior of code designed steel plate shear walls", *Eng. Struct.*, **33**(1), 230-244.
- Berman, J.W. and Bruneau, M. (2005), "Experimental investigation of light-gauge steel plate shear walls", *J. Struct. Eng.*, ASCE, **131**(2), 259-267.
- Bhowmick, A.K. (2009), "Seismic analysis and design of steel plate shear walls", Ph.D. Dissertation, Department of Civil and Environmental Engineering, University of Alberta.
- Bhowmick, A.K., Driver, R.G. and Grondin, G.Y. (2009), "Seismic analysis of steel plate shear walls considering strain rate and P-delta effects", *J. Constr. Steel Res.*, **65**(5), 1149-1159.
- Bhowmick, A.K., Grondin, G.Y. and Driver, R.G. (2011), "Estimating fundamental periods of steel plate shear walls", *Eng. Struct.*, **33**(6), 1883-1893.
- Caccese, V., Elgaaly, M. and Chen, R. (1993), "Experimental study of thin steel-plate shear walls under cyclic load", *J. Struct. Eng.*, ASCE, **119**(2), 573-587.
- Chen, S.J. and Jhang, C. (2006), "Cyclic behavior of low yield point steel shear walls", *Thin-Wall. Struct.*, **44**(7), 730-738.

- Chen, S.J. and Jhang, C. (2011), "Experimental study of low-yield-point steel plate shear wall under in-plane load", *J. Constr. Steel Res.*, **67**(6), 977-985.
- Dung, P.N. (2011), "Seismically retrofitting reinforced concrete moment resisting frames by using expanded metal panels", Ph.D. Dissertation, Structural Engineering Sector, Department of Architecture, Geology, Environment and Constructions, Faculty of Applied Sciences, University of Liege.
- Eatherton, M. (2006), "Design and construction of steel plate shear walls", *Proceedings of the 8th U.S. National Conference on Earthquake Engineering*, Paper No. 588, San Francisco, California, USA.
- FEMA 355C (2000), *State of the Art Report on Systems Performance of Steel Moment Frames Subject to Earthquake Ground Shaking*, Prepared by the SAC Joint Venture for the Federal Emergency Management Agency, Washington, DC.
- Gupta, A. and Krawinkler, H. (1999), *Seismic Demands for Performance Evaluation of Steel Moment Resisting Frame Structures*, Report No. 132, The John A. Blume Earthquake Engineering Center, Department of Civil and Environmental Engineering, Stanford University.
- Habashi, H.R. and Alinia, M.M. (2010), "Characteristics of the wall-frame interaction in steel plate shear walls", *J. Constr. Steel Res.*, **66**(2), 150-158.
- HAZUS-MH MR5 (2010), *Earthquake Loss Estimation Methodology*, Technical and User's Manual, Department of Homeland Security, Federal Emergency Management Agency, Mitigation Division, Washington, DC.
- Kurban, C.O. (2009), "A numerical study on response factors for steel plate shear wall systems", MSc. Thesis, The Graduate School of Natural and Applied Sciences, Middle East Technical University.
- Kurban, C.O. and Topkaya, C. (2009), "A numerical study on response modification, overstrength, and displacement amplification factors for steel plate shear wall systems", *Earthq. Eng. Struct. Dyn.*, **38**(4), 497-516.
- Lubell, A.S. (1997), "Performance of unstiffened steel plate shear walls under cyclic quasi-static loading", MSc. Thesis, Department of Civil Engineering, University of British Columbia, Canada.
- Mahtab, M. and Zahedi, M. (2008), "Seismic retrofit of steel frames using steel plate shear walls", *Asian J. Appl. Sci.*, **1**(4), 316-326.
- Mistakidis, E.S., De Matteis, G. and Formisano, A. (2007), "Low yield metal shear panels as an alternative for the seismic upgrading of concrete structures", *Adv. Eng. Softw.*, **38**(8-9), 626-636.
- Park, H.G., Kwack, J.H., Jeon, S.W., Kim, W.K. and Choi, I.R. (2007), "Framed steel plate wall behavior under cyclic lateral loading", *J. Struct. Eng.*, ASCE, **133**(3), 378-388.
- Rezai, M. (1999), "Seismic behaviour of steel plate shear walls by shake table testing", Ph.D. Dissertation, Department of Civil Engineering, The University of British Columbia, Vancouver, Canada.
- Sabelli, R. and Bruneau, M. (2006), *Steel Plate Shear Walls*, Steel Design Guide 20, American Institute of Steel Construction, Chicago, IL.
- Seilie, I.F. and Hooper, J.D. (2005), "Steel plate shear walls: Practical design and construction", *Modern Steel Constr.*, **45**(4), 37-43.
- Topkaya, C. and Kurban, C.O. (2009), "Natural periods of steel plate shear wall systems", *J. Constr. Steel Res.*, **65**(3), 542-551.